

Study of Wave Load Nonlinearity Effect On Fatigue Life in Component Stochastic Fatigue Analysis

Sungkon Han¹, Kyung-Won Park¹, Hyun-Il Shin¹, and Joo-Ho Heo¹

¹ Daewoo Shipbuilding & Marine Engineering Co. Ltd., Gyeongnam, Korea;
E-mail: skhan2@dsme.co.kr

Abstract

This paper addresses details of wave load nonlinearity effect on stress RAO and damage ratio using component stochastic fatigue analysis. Traditional spectral fatigue analysis for ship structure is based on linear theory; however, there are a number of nonlinearity sources. Especially loading nonlinearity, such as hydrodynamic pressure applying to ship side and gravity changes due to roll and pitch motion, is thought to critically violate the linearity assumption of spectral fatigue analysis, which involves stress RAO as linear parameter. The main focus is placed on how to idealize complicated characteristics of loading nonlinearity and how to implement the nonlinear bias to linear spectral fatigue analysis.

Keywords: component spectral fatigue analysis, loading nonlinearity, stress RAO, gravity change

1 Introduction

This paper deals with nonlinearity correction in spectral fatigue analysis. Spectral fatigue analysis is a typical example applying linear concept towards complicated phenomenon involving stochastic features. Therefore, nonlinearity is neglected or its effect on fatigue life is not appreciated in general due to practical difficulties in implementing it into spectral analysis procedure. Instead, a few simple methods were developed as alliterative measures, in which loading nonlinearity is reflected partly.

Several examples implementing nonlinearities into fatigue analysis procedure are introduced in the present paper and their limitations are reviewed. Loading nonlinearity is known to originate mainly from hydrodynamic pressure applied to ship side and internal pressure due to gravity changes. Their differences in the nonlinear mechanism were not notified clearly from previous applications.

Component spectral fatigue analysis is adopted as the main tool in the present study. It decomposes applied stress into the components induced by hydrodynamic pressure, inertia force on hull and cargo and global loads. Stress influence coefficient is defined by applied stress due to each unit loading component and combined with wave load components to denote resultant dynamic stress. This scheme is shown in equation 1.

$$\sigma_i = \sum_{j=1}^N C_{ij} \cdot f_j \quad (1)$$

where, σ_i is dynamic stress of target location i , C_{ij} is stress influence coefficient and f_j is the j^{th} load component.

Various manipulations are possible by taking advantage of the component spectral analysis. Load components causing nonlinearity can be decomposed from load components involving linear behavior. Time domain simulation was used to find equivalent stress range within the frame work of the component spectral analysis.

2 Nonlinearity sources

There can be many nonlinearity sources in wave load; however, only two sources, in the present study, were dealt with mainly. These are hydrodynamic pressure applying to ship side and dynamic internal pressure induced by gravity changes due to roll and pitch.

2.1 Hydrodynamic pressure on ship side

Most sea keeping analyses for fatigue analysis are based on linear theory and assume small wave amplitude. Hydrodynamic pressure is given only below water line and wave elevation effect is not included. Hydrodynamic pressure coming from wave, however, depends on wave elevation especially at area near water line as shown in Figure 1.

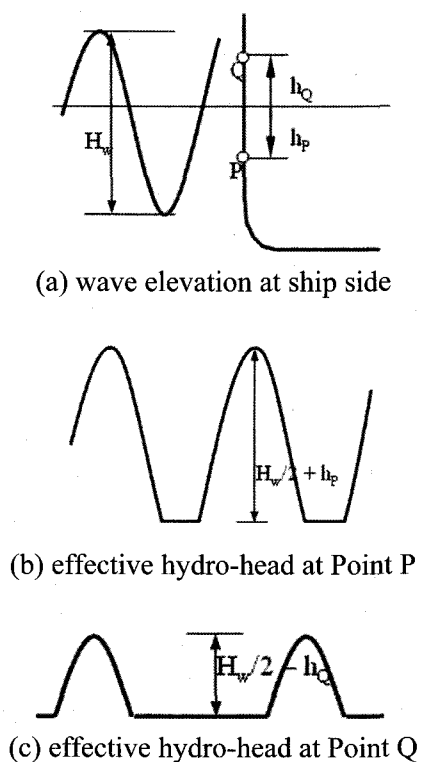


Figure 1: Effective hydro-head depending on wave elevation

Figure 1 shows that hydrodynamic pressure near water line is governed by wave height (H_w) and its location (h_p or h_Q). It is also shown that shipside above water line is subjected to hydrodynamic pressure even though linear solver does not provide pressure at the area.

From DNV's simplified procedure (DNV, 2001) and ABS's spectral fatigue analysis (ABS, 2000), nonlinear correction methods for the side pressure are introduced. The DNV procedure suggests that hydrodynamic pressure be adjusted within the range defined by a representative wave amplitude (z_{wl}) as shown in Figure 2.

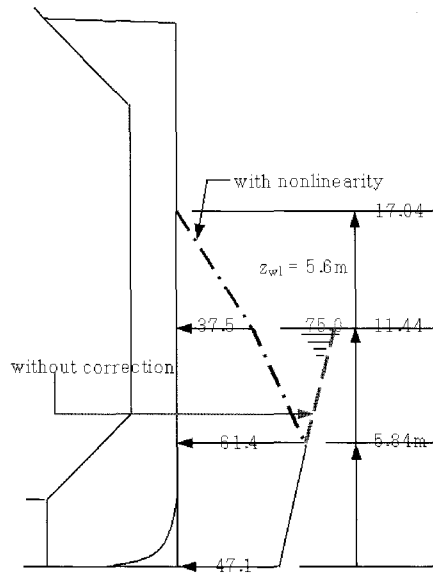


Figure 2: Effective hydro-head depending on wave elevation for a 140K LNGC

A reduction factor linearly varying within the representative wave amplitude is used to correct the nonlinearity effect.

In contrast with the DNV practice, ABS provides a slightly different scheme in its spectral fatigue analysis, which uses dynamic pressure directly from wave load analysis. The reduction factor is defined to be nonlinearly varying only for the area below water line down to 5m as shown in Figure 3, mainly due to its easy implementation.

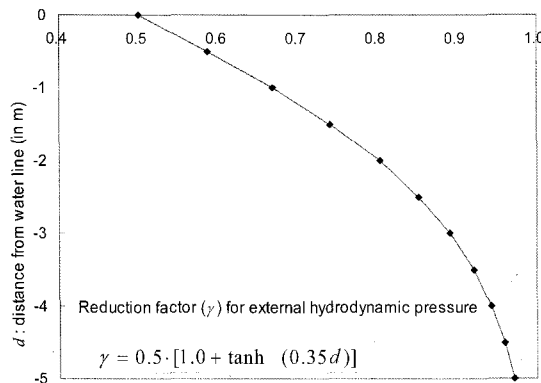


Figure 3: ABS reduction factor for hydrodynamic pressure below water line

Both the DNV and ABS details are found to use a fixed wave amplitude for simplicity rather than to adopt wave height dependent reduction factor.

2.2 Dynamic internal pressure due to motion

Internal pressure induced by liquid cargo is one of the most ambiguous areas from the fact that ship motion involves highly nonlinear liquid motion. This dynamic internal pressure has been modeled using quasi-static concept excluding any complicated deviation from the simple idealization. There are two types of idealization regarding dynamic internal pressure due to ship motion as shown in Figure 4 (Violette, 1997).

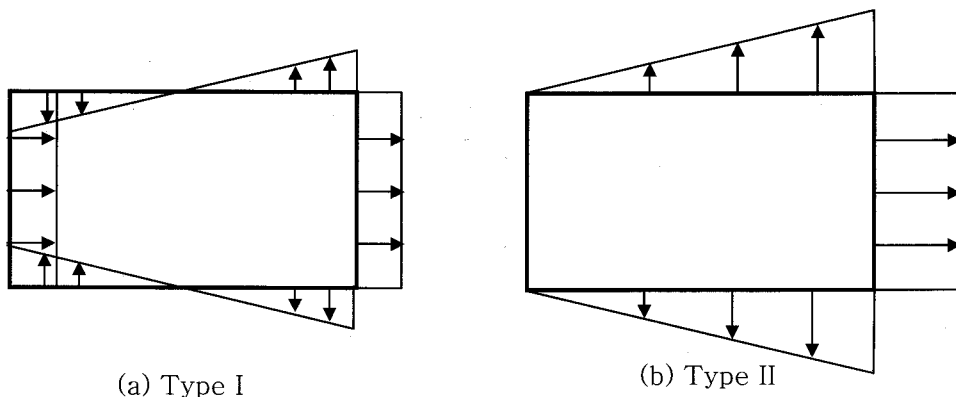


Figure 4: Dynamic internal pressure types due to ship motion

Type I in Figure 4 is considered to be free from nonlinearity because of its anti-symmetry loading pattern; however Type II is thought to cause nonlinear stress fluctuation. Rotation motion such as roll and pitch causes change in gravity direction and induces dynamic internal pressure consequently. This component is also idealized to induce dynamic internal pressure of Type II.

ABS adopts Type II internal pressure in its spectral fatigue analysis but DNV uses Type I in its simplified fatigue analysis procedure without distinguishing gravity change from transitional accelerations. In its procedure, Classification Notation 30.7, equivalent translation acceleration is calculated incorporating gravity change component “ $g_o \sin \phi$ ” as in equation 2.

$$a_t = \sqrt{a_y^2 + (g_o \sin \phi + a_{ry})^2} \quad (2)$$

where a_t is resultant transverse acceleration, a_y acceleration due to sway and yaw, g_o gravitational constant, ϕ roll angle and a_{ry} horizontal component of roll acceleration. Therefore the DNV method does not contain nonlinearity in its resultant stress fluctuation.

A component spectral fatigue analysis system developed by DSME adopts combined scheme of Types I and II. Internal pressure Type I is used for the acceleration due to sway and yaw and Type II is adopted to simulate dynamic internal pressure induced by gravity change due to roll.

Internal pressure Type II induces stress fluctuation that is very different from sinusoidal function as depicted in Figure 5, which is for roll motion.

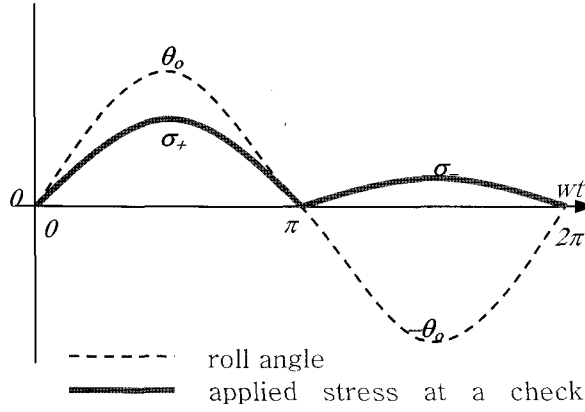


Figure 5: Stress fluctuation induced by internal pressure Type II in Figure 4

The nonlinearity from motion is not a function of wave height, which is different from hydrodynamic pressure on side shell. Actual stress range can be very different from the value calculated based on the linear basis.

3 Correction for nonlinearity in component spectral fatigue analysis

Component spectral fatigue analysis has its strong point in that each component can be dealt with separately. In general, stress in hull structure of liquid cargo vessels is determined by combination of hull girder loading, external hydrodynamic pressure and internal pressure due to ship motion. The internal pressure can be again decomposed into resultant translational acceleration and gravity change components. Therefore, dynamic stress at a check point j , σ_j can be given by Equation 3:

$$\sigma_j = \sum_i f_{ij} P_i + \sum_i g_{ij} a_i + \sum_i h_{ij} M_i + \sum_i k_{ij} \phi_i \quad (3)$$

where

- P_i : hydrodynamic pressure
- a_i : acceleration
- M_i : global loads – bending moments & shear forces
- ϕ_i : roll and pitch angle
- f_{ij}, g_{ij}, h_{ij} and k_{ij} : stress influence coefficients, respectively.

Equation 3 can be rewritten to Equation 4 in terms of time t and wave height H_w , considering time variation.

$$\begin{aligned} \sigma_j(t, H_w) = & \sum_i f_{ij} P_i(t, H_w) + \sum_i g_{ij} a_i(t, H_w) \\ & + \sum_i h_{ij} M_i(t, H_w) + \sum_i k_{ij} \phi_i(t, H_w) \end{aligned} \quad (4)$$

where loading components a_i and M_i are assumed to be linear in the present study. Nonlinearity involved in hydrodynamic pressure can be idealized as follows:

For $(H_w / 2) > |h|$

$$P(t, H_w) = \max \left\{ \begin{array}{l} P_o \cos(\omega t - \varphi) - P_{ref} \\ 0 \end{array} \right\} \quad (5)$$

otherwise $P(t, H_w) = P_o \cos(\omega t + \varphi)$ (6)

where,

$$P_o = \left(\frac{H_w}{2} \right) \sqrt{P_{real}^2 + P_{imag}^2}$$

$$\varphi = \tan^{-1} \left(\frac{P_{imag}}{P_{real}} \right)$$

$$P_{ref} = P_o h / (H_w / 2)$$

h : distance from water line as shown in Figure 1, positive upward.

With given stress influence coefficient f_{ij} , varying dynamic pressure P_i is determined according to Equations 5 and 6 to define fluctuation of applied stress.

For the gravity change term in Equation 4, similar correction is required considering the stress fluctuation depicted in Figure 5. In that case no nonlinear aspect is involved in loading $\phi_i(t, H_w)$. Instead, stress influence coefficient k_{ij} should be replaced by k_{ij}^+ and k_{ij}^- , considering the sign of the loading component $\phi_i(t, H_w)$. This modification is given as follows:

$$k_{ij} \phi_i \Rightarrow \begin{cases} k_{ij}^+ \phi_i(t, H_w) & \phi_i(t) \geq 0 \\ k_{ij}^- \phi_i(t, H_w) & \phi_i(t) < 0 \end{cases} \quad (7)$$

where

$$k_{ij}^+ = \sigma_+ / \theta_o, \quad k_{ij}^- = \sigma_- / \theta$$

$$\phi_i(t) = (H_w / 2) \cdot \sqrt{\phi_{i,real}^2 + \phi_{i,imag}^2} \cos(\omega t + \varphi) \quad \varphi = \tan^{-1} \left(\frac{\phi_{i,imag}}{\phi_{i,real}} \right)$$

Stress fluctuation, for a given H_w , is given according to Equation 4, taking into account nonlinearities coming from Equations. 5~7. Resultant stress range is obtained from the simulated stress fluctuation in time domain as shown in Figure 6.

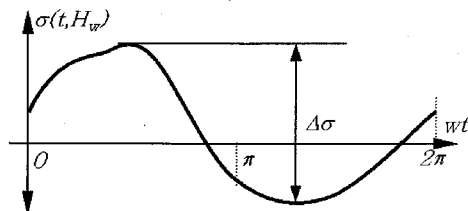


Figure 6: Stress range in a non-sinusoidal function

Stress RAO is given by:

$$\sigma_{RAO} = \Delta\sigma / H_w \quad (8)$$

The stress RAO obtained by this is used for spectral fatigue analysis later; however, it is to be noted that the stress RAO varies for wave height. This aspect should be adequately considered in short term response calculation, where a significant wave height is given for a specific sea state.

4 Results and discussion

A sample fatigue analysis was carried out for a 140,000m³ LNG carrier for quantitative study on nonlinearity correction effect. Figure 7 shows an FE model, check points and coordinate system used for this case study.

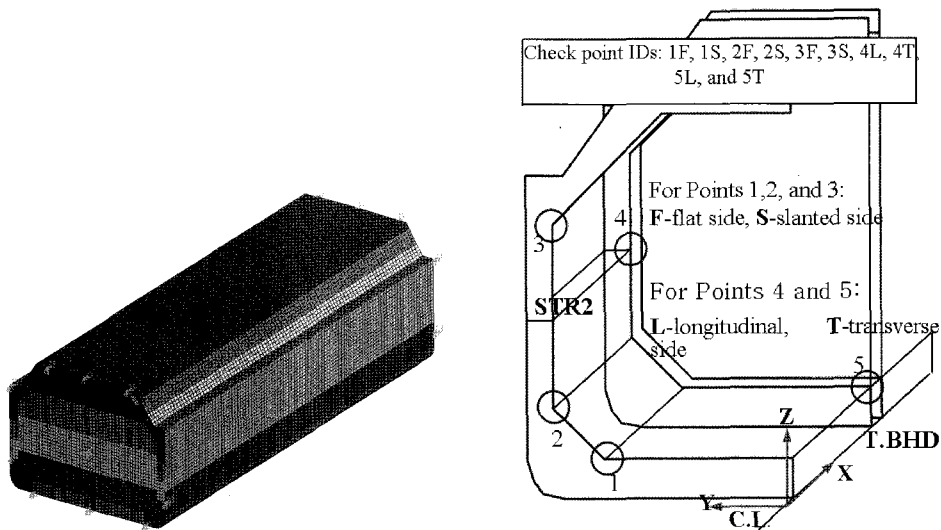


Figure 7: FE model, Check Point IDs and coordinate convention

Wave load analysis was carried out using KR3-D, which was developed based on 3-D panel method by KR. Stress RAO is used for detailed comparison. Stress RAOs at **Point 1F** are shown in Figure 8 for a few heading angles – 0, 80, 100, 180, 260 and 280 degrees. It is seen from Figure 8 that nonlinearity correction reduces stress RAO. This reduction is outstanding especially for beam sea condition.

To analyze the reduction in more detail, stress RAO is decomposed into each term as given in Equation 3 and only the two components involving nonlinearity – hydrodynamic pressure and gravity change – are compared in Figure 9 to see how much nonlinearity correction effects stress RAO.

Figure 9 shows that reduction in stress RAO is significant for gravity component and the stress RAOs of each beam sea set (80 and 280, 100 and 260 degrees) become the same. External-pressure-induced stress RAO shows noticeable reduction only in the beam sea conditions.

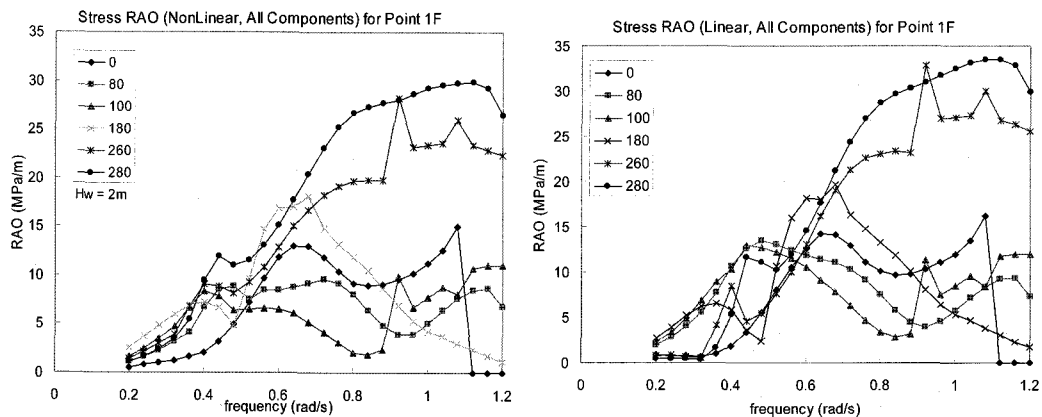


Figure 8: Stress RAO comparison between linear and nonlinear ($H_w=2.0m$) cases

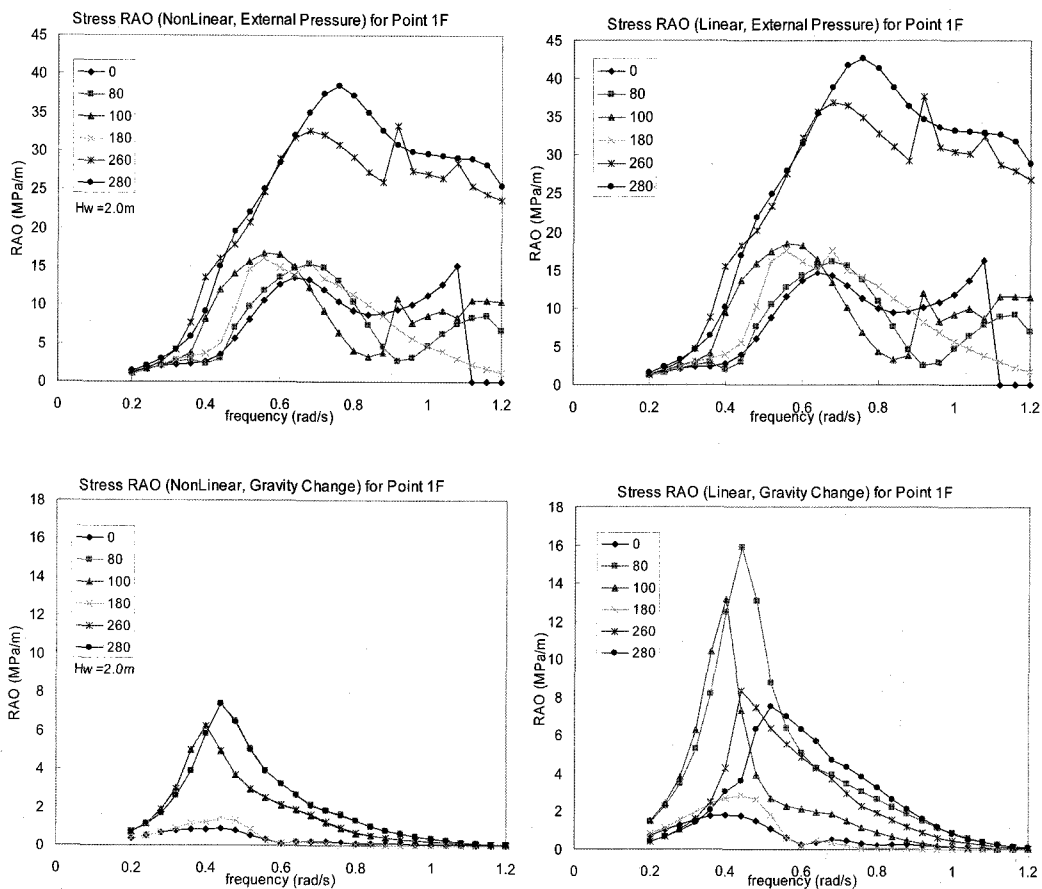


Figure 9: Component Stress RAO comparison between linear and nonlinear ($H_w=2.0m$) cases

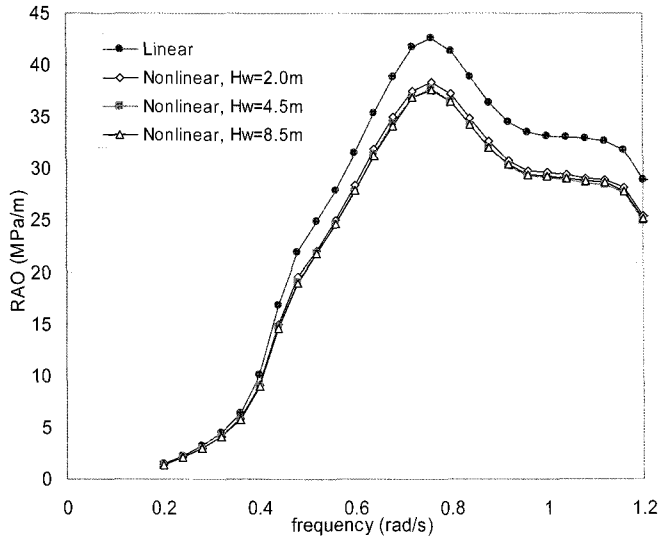


Figure 10: External Pressure induced stress RAO for **Point 1F**; Heading 280°

External-pressure-induced stress RAOs for heading 280° are compared in Figure 10 for different wave heights to see the effect of wave height. Stress RAO, in general, is observed to become smaller with higher wave height, but only to a little extent.

External pressure induced stress RAOs of heading 280° are compared for **Points 1F** and **3F** in Figure 11. Effect of nonlinearity correction is the same for the two points and external pressure is seen to be more dominant at Point 1F than Point 3F, as easily expected.

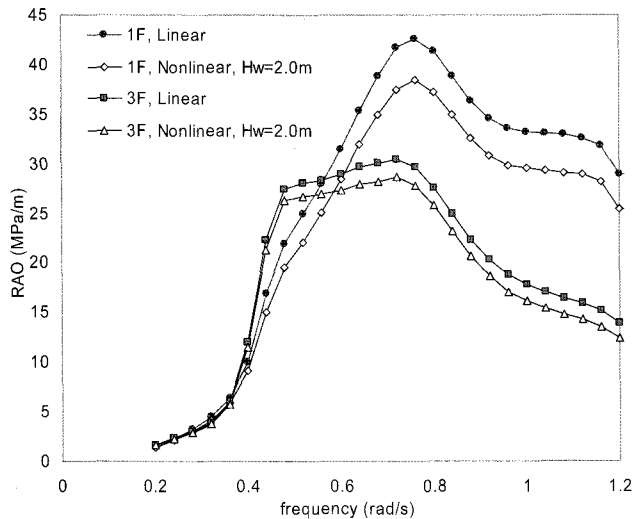


Figure 11: External pressure induced stress RAO for **Points 1F** and **3F**; Heading 280°

Gravity change induced stress RAOs for heading 80° are compared for **Points 1F**, **2F** and **3F** in Figure 12. This gravity change comes from roll rather than pitch because of the beam sea condition. Internal pressure Type II in Figure 4 is the source of applied stress and the upper knuckle of **Point 3F** is seen to be the most vulnerable to this component.

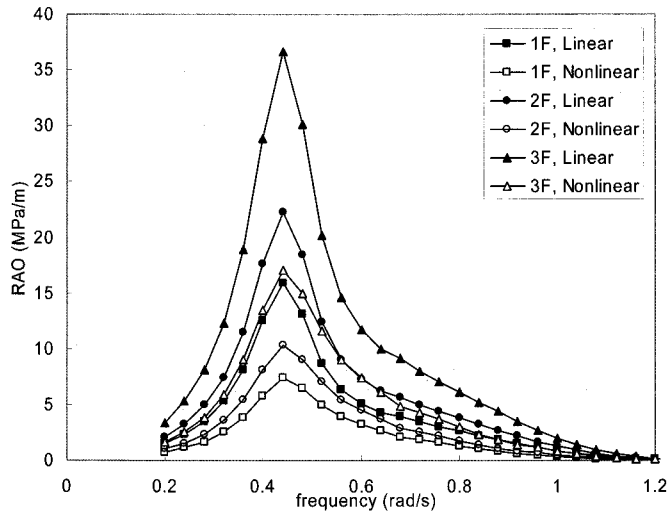


Figure 12: Gravity change induced stress RAO for **Points 1F, 2F, and 3F**; Heading 80°

Whether to apply nonlinearity correction is seen to make a big difference in stress RAO value; therefore, a proper care should be taken to get more realistic fatigue damage ratio.

Gravity change induced stress RAOs for heading 80° are compared for **Points 4L** and **5L** in Figure 13. Similar trend to hopper connections compared in Figure 12 is shown. Side structure (**Point 4L**) is subjected to higher stress due to gravity change than center structure (**Point 5L**). **Points 4L** and **5L** are located near transverse bulkhead and pitch effect is included. Nonlinearity corrected stresses are seen to be higher stress at high frequency range (over 0.6 rad/s) than linear stress RAOs due to pitch effect.

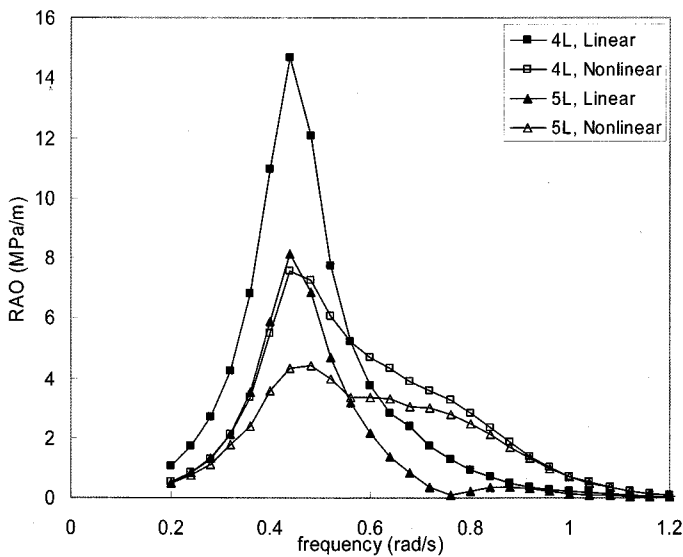


Figure 13: Gravity change induced stress RAO for **Points 4L** and **5L**; Heading 80°

Fatigue life comparison for the check points of Figure 7 is made in Table 1.

Table 1: Comparison of fatigue life between linear and nonlinear cases (years)

Check Point	Linear	Nonlinear
1F	21.8	32.0
1S	51.2	74.2
2F	97.5	101.0
2S	183.0	182.0
3F	87.0	98.7
3S	51.1	57.4
4L	225	174
4T	345	180
5L	302	346
5T	178	194

Table 1 shows that nonlinear correction reduces fatigue life for **Points 4L** and **4T** differently from other points. This can be explained with Figure 14 comparing each component and total combined stress RAOs between linear and nonlinear cases. It shows that the area enclosed by total combined stress RAO is increased for the nonlinear correction case, which finally gives low fatigue life.

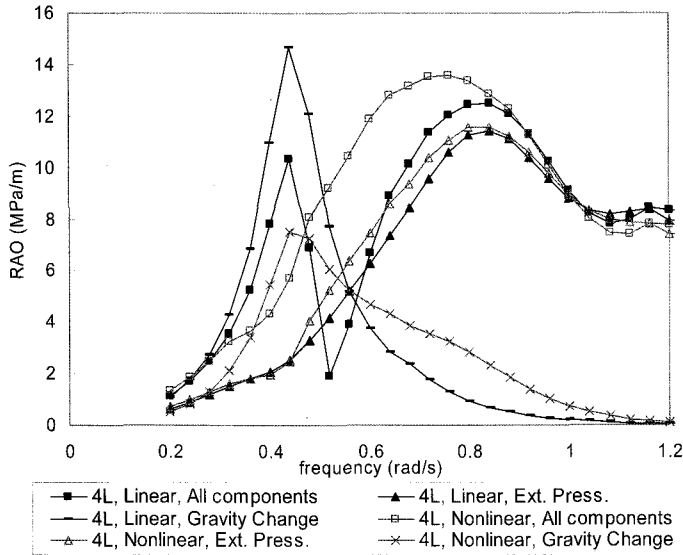


Figure 14: Stress RAO comparison for **Point 4L**; Heading 80°, Nonlinear correction for $H_w=2.0m$

5 Conclusion remarks

Loading nonlinear effect is successfully incorporated to the component spectral fatigue analysis system, developed by DSME, through the decomposition of stress component and time domain simulation taking into account nonlinear aspect involved to external pressure applied to ship side and gravity change due to roll and pitch motions. External pressure on

ship side induces nonlinear fluctuation depending on distance from water line and wave height. Gravity change due to ship motion induces nonlinearity depending on the sign of a considered motion component, roll or pitch.

The effect of nonlinearity involved in external pressure is found to reduce equivalent stress RAO compared to that calculated based on linear assumption. It is seen that with higher wave height, equivalent stress RAO becomes smaller, but only to a limited extent.

Gravity changes with internal pressure Type II in Figure 4 is found to bring great differences between linear and nonlinear cases. This observation is explained from the fact that the sign of applied stress does not change in the same manner as motion – roll and pitch. This aspect is well depicted in Figure 5. Nonlinearity involved in gravity change should be implemented especially for side knuckles of LNG carriers since the nonlinear correction gives quite different stress RAOs as shown Figure 12.

It is shown that nonlinearity correction can, in some case, increase stress RAO especially for the area near water line. This is shown from Figure 14, showing comparison result of stress RAOs between linear and nonlinear cases for No.2 Stringer connection at transverse bulkhead.

References

- American Bureau of Shipping, April 2000 Procedure for Spectral Fatigue Analysis.
Det Norske Veritas. 2001. Fatigue Assessment of Ship Structure. Classification Notes, **30**.
7.
Violette, F.L.M. 1997. On the Fatigue Performance Prediction of Ship Structural Details.
University of Southampton, PhD Thesis.